

GaMnAs-based hybrid multiferroic memory device

M. Overby,¹ A. Chernyshov,¹ L. P. Rokhinson,¹ X. Liu,² and J. K. Furdyna²

¹*Department of Physics and Birck Nanotechnology Center,
Purdue University, West Lafayette, Indiana 47907 USA*

²*Department of Physics, University of Notre Dame, Notre Dame, Indiana 46556 USA*

(Dated: April 26, 2019)

A rapidly developing field of spintronics is based on the premise that substituting charge with spin as a carrier of information can lead to new devices with lower power consumption, non-volatility and high operational speed^{1,2}. Despite efficient magnetization detection^{3,4,5}, magnetization manipulation is primarily performed by current-generated local magnetic fields and is very inefficient. Here we report a novel non-volatile hybrid multiferroic memory cell with electrostatic control of magnetization based on strain-coupled GaMnAs ferromagnetic semiconductor⁶ and a piezoelectric material. We use the crystalline anisotropy of GaMnAs to store information in the orientation of the magnetization along one of the two easy axes, which is monitored via transverse anisotropic magnetoresistance⁷. The magnetization orientation is switched by applying voltage to the piezoelectric material and tuning magnetic anisotropy of GaMnAs via the resulting stress field.

In magnetic memories the information is stored in the orientation of magnetization. The major weakness of current MRAM implementations lies in the inherently non-local character of magnetic fields used to flip ferromagnetic domains during the write operation. Neither thermal switching⁸ nor current induced switching⁹ can solve the problem completely.

An attractive alternative to conventional ferromagnets are multiferroic materials¹⁰, where ferromagnetic and ferroelectric properties coexist and magnetization can be controlled electrostatically via magnetoelectric coupling. In single-phase and mixed-phase multiferroics ferromagnetic material must be insulating in order to avoid short-circuits. Alternatively, magnetoelectric coupling can be introduced between ferromagnetic and ferroelectric materials indirectly via strain, and in this case the ferromagnetic material can be conducting. A conceptual memory device made of ferromagnetic and piezoelectric materials has been proposed¹¹, and permeability changes in magnetostrictive films¹², changes in coercive field¹³ and re-orientation of the easy axis from in-plane to out-of-plane in Pd/CoPd/Pd trilayers¹⁴ have been recently demonstrated.

Some ferromagnetic materials have a complex anisotropic magnetocrystalline energy surface and several easy axes of magnetization. If the energy barrier between adjacent easy-axis states can be controlled by strain, then a multiferroic non-volatile multi-state mem-

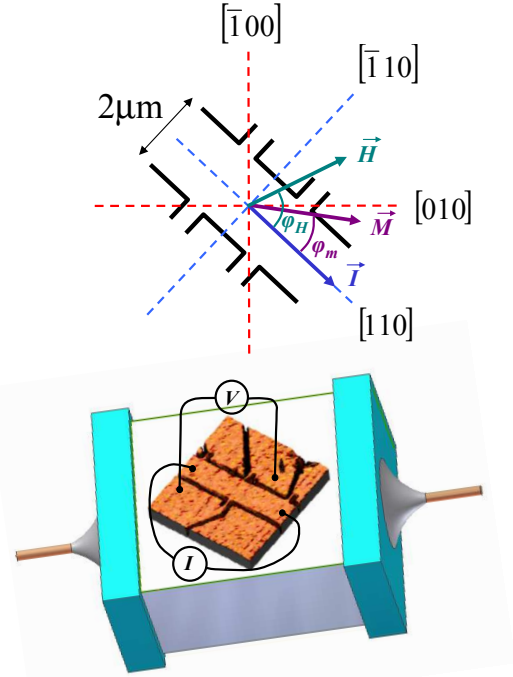


FIG. 1: Top: sketch of the Hall bar with relative orientation of electrical current \vec{I} , magnetic field \vec{H} and magnetization \vec{M} . Bottom: an AFM image of a $2\mu\text{m}$ -wide Hall bar is schematically shown attached to the piezoelectric. Strain is applied to the sample along $[100]$ and $[010]$ directions, red dashed lines on the sketch.

ory device can be realized. Magnetic anisotropy of dilute magnetic semiconductor GaMnAs films is largely controlled by epitaxial strain^{15,16}, with compressive (tensile) strain inducing in-plane (out-of-plane) orientation of magnetization. In GaMnAs compressively strained to (001) GaAs there are two equivalent easy axes of in-plane magnetization: along $[100]$ and along $[010]$ crystallographic directions. Lithographically-induced unidirectional lateral relaxation can be used to select the easy axis^{17,18}. In addition to the large in-plane crystalline anisotropy there is an uniaxial anisotropy between $[110]$ and $[1\bar{1}0]$ directions which is probably due to the underlying anisotropy of the reconstructed GaAs surface¹⁹. We use this magnetocrystalline anisotropy in combination with the magnetostrictive effect to demonstrate a bi-stable memory device.

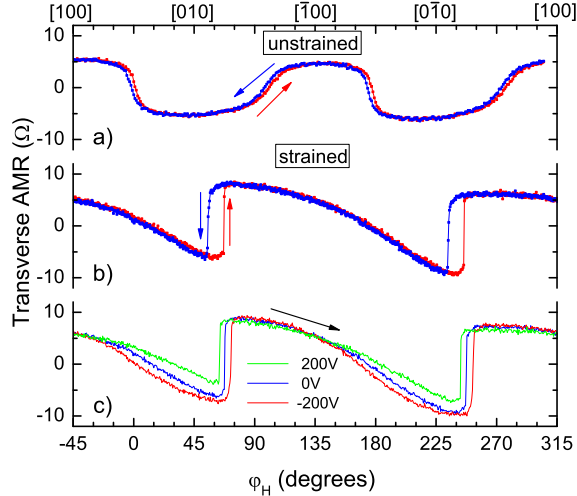


FIG. 2: Transverse AMR as a function of magnetic field angle φ_H for unstrained (a) and strained (b,c) samples. Arrows indicate the field sweep directions. Magnetic field is $H = 50$ mT and $T = 35$ K. Voltage applied to the piezoelectric $V_{pzt} = 0$ for the curves (b) and $V_{pzt} = \pm 200$ V and 0 for (c).

Molecular beam epitaxy at 265° C was employed to grow 15-nm thick epilayers of $\text{Ga}_{0.92}\text{Mn}_{0.08}\text{As}$ on semi-insulating (001) GaAs substrates. The wafers were subsequently annealed for 1 hour at 280° C in a nitrogen atmosphere. Annealing increases the Curie temperature of the ferromagnetic film to $T_c \sim 80$ K and reduces the cubic anisotropy. The GaMnAs layer was patterned into $2 \mu\text{m}$ -wide Hall bars oriented along the $[110]$ axis by combination of e-beam lithography and wet etching, see Fig. 1. After lithography $3 \text{ mm} \times 3 \text{ mm}$ samples were mechanically thinned to $\sim 100 \mu\text{m}$ and attached to a multilayer PZT (piezoelectric lead-zirconium-titanate ceramic)²⁰ with epoxy, aligning the $[010]$ axis with the axis of polarization of the PZT. Application of positive (negative) voltage V_{PZT} across the piezoelectric introduces tensile (compressive) strain in the sample along the $[010]$ direction, and strain with the opposite sign along the $[100]$ direction proportional to the piezoelectric strain coefficients $d_{33} \approx -2d_{31}$. Both coefficients decrease by a factor of 15 between room temperature and 4.2 K. The induced strain $\varepsilon = \Delta L/L$ for both $[010]$ and $[100]$ directions was monitored with a biaxial strain gauge glued to the bottom of the piezoelectric. Strain is proportional to the change of the gauge resistance, and was measured in the Wheatstone bridge configuration: $\Delta\varepsilon = \varepsilon_{[010]} - \varepsilon_{[100]} = (\Delta L/L)_{[010]} - (\Delta L/L)_{[100]} = \alpha(R_{[010]} - R_{[100]})/R$, where α is the gauge sensitivity coefficient and R is the resistance of the unstrained gauge. It has been shown before²¹ that the strain gradient across the piezoelectric and the sample is negligible: i.e., gauges glued on top of the sample and on the opposite side of the piezoelectric measure

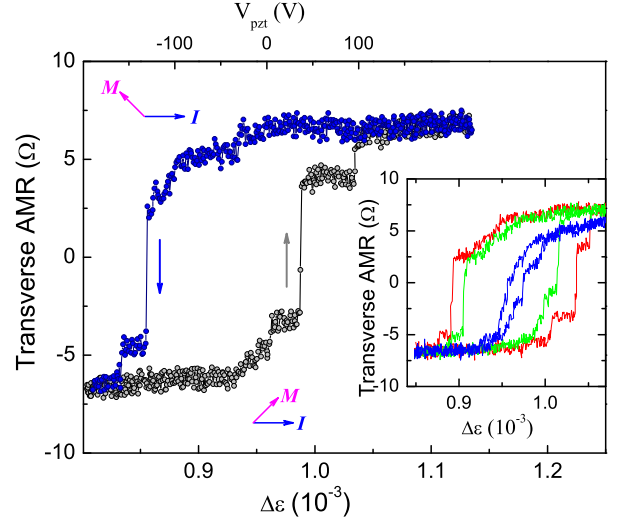


FIG. 3: Transverse AMR (TrAMR) for the strained Hall bar as a function of uniaxial strain measured by a strain gauge. Static magnetic field $H = 50$ mT is applied at $\varphi_H = 62^\circ$, the data is taken at $T = 35$ K. On the top axis approximate voltage on the piezoelectric is indicated. Orientation of magnetization relative to the current flow is shown schematically for the $\text{TrAMR} > 0$ and $\text{TrAMR} < 0$ states. In the inset TrAMR is plotted for $H = 50$ mT (red), 70 mT (green) and 100 mT (blue) measured at $T = 25$ K.

similar strain.

Direction of the in-plane magnetization \vec{M} is measured via transverse anisotropic magnetoresistance (TrAMR), also known as giant planar Hall effect⁷

$$\text{TrAMR} = (\rho_{\parallel} - \rho_{\perp}) \sin \varphi_m \cos \varphi_m, \quad (1)$$

where ρ_{\parallel} and ρ_{\perp} are the resistivities for magnetization oriented parallel and perpendicular to the current. The sign and magnitude of TrAMR depend on the angle φ_m between magnetization \vec{M} and current $\vec{I} \parallel [110]$, see schematic in Fig. 1. TrAMR reaches minimum (maximum) when $\vec{M} \parallel [010]$ ($\vec{M} \parallel [\bar{1}00]$). Longitudinal AMR is $\propto \cos^2 \varphi_m$ and is not sensitive to the magnetization switching between 45° and 135° .

In Fig. 2 TrAMR is plotted for the strained and unstrained Hall bars as magnetic field of constant magnitude $H = 50$ mT is rotated in the plane of the sample. For the unstrained sample (not attached to the piezoelectric) there are four extrema for the field angle φ_H around 45° , 135° , 225° and 315° with four switchings of magnetization by 90° near $[110]$ and $[\bar{1}\bar{1}0]$ directions, which reflects the underlying crystalline anisotropy of GaMnAs. For the sample attached to the piezoelectric there is a gradual change in the angle of magnetization with only two abrupt 90° switchings of the direction of magnetization per field rotation, which indicates strong uniaxial anisotropy due to a highly anisotropic thermal

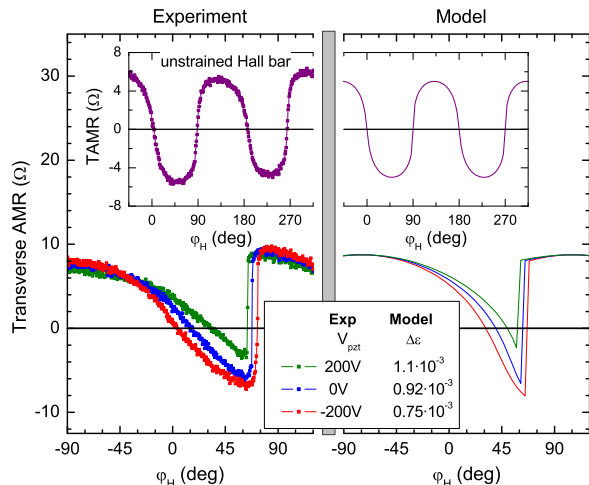


FIG. 4: Experimentally measured (left panel) and modelled (right panel) transverse AMR for the strained sample at different voltages on the piezoelectric (for comparison data for an unstrained sample are shown in the inset). All data were taken at $T = 35$ K and $H = 50$ mT. In the model we used experimentally measured strain $\Delta\epsilon$, other model parameters are discussed in the text.

expansion coefficient of the PZT stack (+1 ppm/K along and -3 ppm/K perpendicular to the piezoelectric stack). By applying a finite voltage to the piezoelectric during cooldown we are able to control the thermally-induced stress within $\Delta\epsilon < 10^{-3}$ for $T < 50$ K.

Application of ± 200 volts on the piezoelectric results in a shift of the angle of magnetization switching by $\Delta\varphi_H \approx 10^\circ$, which is comparable to the size of the hysteresis loop in TrAMR vs φ_H scans at $V_{pzt} = 0$, Fig. 2(b,c). Applying a magnetic field of $H = 50$ mT oriented at $\varphi_H = 62^\circ$, which corresponds to the middle of the hysteresis loop, compensates for the thermally induced uniaxial strain anisotropy and restores the original degeneracy between $[010]$ and $[\bar{1}00]$ magnetization directions of the unstrained GaMnAs for $V_{pzt} \approx 0$. An additional strain is then applied by varying voltage on the piezoelectric. In Fig. 3 TrAMR is plotted as a function of measured strain $\Delta\epsilon$, the corresponding V_{pzt} are approximately marked on the top axis (there is a small hysteresis in $\Delta\epsilon$ vs V_{pzt}). As additional compressive strain is applied along $[010]$, this direction becomes the easy axis of magnetization and magnetization aligns itself with $[010]$. As additional tensile strain is applied along $[010]$ direction, the $[\bar{1}00]$ direction becomes the easy axis and polarization switches by 90° . The switching occurs in a few steps, indicating a few-domain composition of our device. At $V_{pzt} = 0$ the magnetization has two stable orientations, $\vec{M} \parallel [\bar{1}00]$ and $\vec{M} \parallel [010]$, and the orientation can be switched by applying a negative or a positive voltage on the piezoelectric. Thus, the device performs as a bi-stable

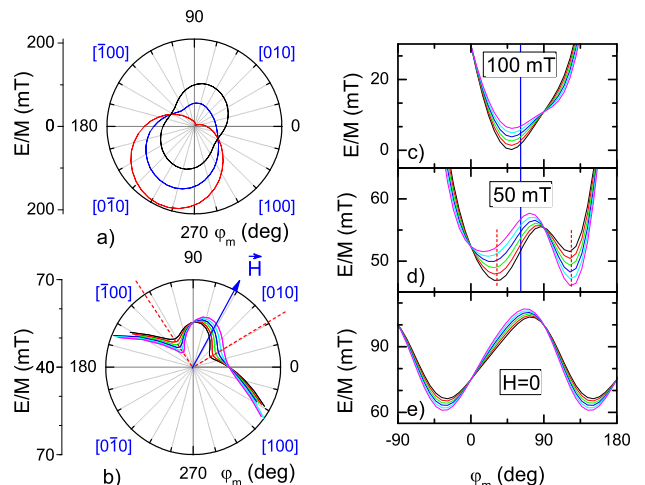


FIG. 5: a) Polar plot of magnetostatic energy E/M as a function of magnetization angle φ_m for $H = 0$ (black), 50 mT (blue) and 100 mT (red) for $\varphi_H = 62^\circ$ and $V_{pzt} = 0$ ($\Delta\epsilon K_\epsilon = 16$ mT). b-d) Angular dependence of E/M for $\Delta\epsilon K_\epsilon = 13$ –19 mT (black to magenta) for $H = 0$ (e), $H = 50$ mT (b,d) and $H = 100$ mT (c). Blue line and arrow mark $\varphi_H = 62^\circ$, dashed red lines indicate two stable orientations of magnetization.

non-volatile magnetic memory with electrostatic control of the state.

The center of the loop can be shifted by adjusting φ_H : e.g., a 1° change shifts the center of the loop by $\Delta\epsilon \approx 3.5 \cdot 10^{-5}$. As H increases, the size of the hysteresis loop decreases, and the hysteresis vanishes for $H > 100$ mT; see inset in Fig. 3. At $H < 40$ mT the loop increases beyond the ± 200 piezoelectric voltage span. In our experiments the magnetic field balances the residual strain due to anisotropic thermal expansion of the PZT. Alternatively, intrinsic piezoelectric properties of GaAs can be utilized, in this case there will be no thermally induced strain and electrostatic switching of the magnetization direction can be realized without applying an external compensating magnetic field. Scaling of the piezoelectric element from 0.5 mm down to $\sim 1 \mu\text{m}$ will compensate for a small strain coefficient in GaAs ($d_{33}^{pzt} \approx 10 \cdot d_{14}^{GaAs}$ at 30 K), reduce operating voltage to a few volts and allow electrostatic control of individual memory cells.

We model the strain along $[100]$ and $[010]$ directions as an extra magnetostatic energy density term $2\epsilon_{[100]}K_\epsilon \sin^2(\varphi_m + 45^\circ) + 2\epsilon_{[010]}K_\epsilon \sin^2(\varphi_m - 45^\circ) = \Delta\epsilon K_\epsilon \sin(2\varphi_m) + const.$ Then, for a single domain magnet the free energy density can be written as

$$E = K_u \sin^2(\varphi_m) + K_1/4 \cos^2(2\varphi_m) + HM \cos(\varphi_m - \varphi_H) + \Delta\epsilon K_\epsilon \sin(2\varphi_m) \quad (2)$$

omitting constant offset, where K_1 , K_u and K_ϵ are cubic, uniaxial and strain anisotropy constants; H is the applied in-plane magnetic field; and φ_m and φ_H are the angles

between [110] direction and magnetization and magnetic field respectively; see schematic in Fig. 1. We assume that K_ε is the same for [100] and [010] directions.

In equilibrium the magnetization orientation φ_m minimizes the free energy, $dE/d\varphi_m = 0$ and $d^2E/d\varphi_m^2 > 0$. The TrAMR can be calculated from Eq. 1 for a given angle φ_H of the external field H . From the fits to the experimental TrAMR data we can extract the anisotropy constants K_1 , K_u and K_ε . The model captures all the essential features of the data, and corresponding fits are shown in Fig. 4 for the strained and unstrained devices. For unstrained device anisotropy fields $2K_1/M = 40$ mT and $2K_u/M = 6$ mT. These values are significantly smaller than the previously reported values for as-grown (not annealed) wafers^{7,22}. For the sample attached to the piezoelectric the crystalline anisotropy field remains the same, but the uniaxial anisotropy increases to $2K_u/M = 50$ mT. The strain-induced anisotropy field $\Delta\varepsilon K_\varepsilon/M$ varies between 13 mT and 19 mT for different V_{pzt} between -200 V and 200 V, the coefficient $K_\varepsilon/M = 17$ T.

To illustrate the mechanism of magnetization switching we plot magnetic energy density normalized by magnetization E/M (Eq. 2) as a function of φ_m in Fig. 5. At $H = 0$ there are only two minima along the [100] axis due to the large uniaxial strain (see Fig. 5 (a,e)), caused by anisotropic thermal expansion coefficient of the piezoelectric.

With external magnetic field $H = 50$ mT applied at $\varphi_H = 62^\circ$ E/M has two minima: at $\varphi_m = 32^\circ$ and at 123° , i.e., close to [010] and to $[\bar{1}00]$ crystallographic directions. For the strain field $\Delta\varepsilon K_\varepsilon/M = 13$ mT the global minimum is at $\varphi_m = 32^\circ$, and in equilibrium the magnetization is oriented along the [010] direction. As the strain field increases to 19 mT the two minima switch, and $\varphi_m = 123^\circ$ becomes the global minimum. It is interesting to note that there is always a small barrier between the two minima. Unless the barrier is an artifact of our model, the switching of magnetization should be either temperature activated or should occur via macroscopic quantum tunnelling.

-
- ¹ G. A. Prinz, Magnetoelectronics. *Science* **282**, 1660-1663 (1998).
 - ² S. A. Wolf *et al.*, Spintronics: a spin-based electronics vision for the future. *Science* **294**, 1488 (2001).
 - ³ M. Baibich *et al.*, Giant magnetoresistance of (001)Fe/(001)Cr magnetic superlattices. *Phys. Rev. Lett.* **61**, 2472 (1988).
 - ⁴ G. Binasch, P. Grünberg, F. Saurenbach, and W. Zinn, Enhanced magnetoresistance in layered magnetic structures with antiferromagnetic interlayer exchange. *Phys. Rev. B* **39**, 4828-4830 (1989).
 - ⁵ J. Moodera, L. Kinder, T. Wong, and R. Meservey, Large magnetoresistance at room temperature in ferromagnetic thin film tunnel junctions. *Phys. Rev. Lett.* **74**, 3273 (1995).
 - ⁶ H. Ohno, Making nonmagnetic semiconductors ferromagnetic. *Science* **281**, 951 - 6 (1998).
 - ⁷ H. Tang, R. Kawakami, D. Awschalom, and M. Roukes, Giant planar Hall effect in epitaxial (Ga,Mn)As devices. *Phys. Rev. Lett.* **90**, 107201 - 1 (2003).
 - ⁸ M. Kerekes *et al.*, Dynamic heating in submicron size magnetic tunnel junctions with exchange biased storage layer. *J. Appl. Phys.* **97**, 10 - 501 (2005).
 - ⁹ E. Myers *et al.*, Current-induced switching of domains in magnetic multilayer devices. *Science* **285**, 867 - 70 (1999).
 - ¹⁰ W. Eerenstein, N. Mathur, and J. Scott, Multiferroic and magnetoelectric materials. *Nature* **442**, 759 - 65 (2006).
 - ¹¹ V. Novosad *et al.*, Novel magnetostrictive memory device. *J. Appl. Phys.* **87**, 6400 - 2 (2000).
 - ¹² K. Arai, C. Muranaka, and M. Yamaguchi, A new hybrid device using magnetostrictive amorphous films and piezoelectric substrates. *IEEE Trans. Magn.* **30**, 916 - 18 (1994).
 - ¹³ H. Boukari *et al.*, Voltage assisted magnetic switching in $\text{Co}_{50}\text{Fe}_{50}$ interdigitated electrodes on piezoelectric substrates. *J. Appl. Phys.* **101**, 54903 - 1 (2007).
 - ¹⁴ J.-W. Lee, S.-C. Shin, and S.-K. Kim, Spin engineering of CoPd alloy films via the inverse piezoelectric effect. *Appl. Phys. Lett.* **82**, 2458 - 60 (2003).
 - ¹⁵ U. Welp *et al.*, Magnetic Domain Structure and Magnetic Anisotropy in $\text{Ga}_{1-x}\text{Mn}_x\text{As}$. *Phys. Rev. Lett.* **90**, 167206 (2003).
 - ¹⁶ X. Liu, Y. Sasaki, and J. K. Furdyna, Ferromagnetic resonance in $\text{Ga}_{1-x}\text{Mn}_x\text{As}$: Effects of magnetic anisotropy. *Phys. Rev. B* **67**, 205204 (2003).
 - ¹⁷ S. Hümpfner *et al.*, Lithographic engineering of anisotropies in (Ga,Mn)As. *Appl. Phys. Lett.* **90**, 102102 (2007).
 - ¹⁸ J. Wenisch *et al.*, Control of Magnetic Anisotropy in (Ga,Mn)As by Lithography-Induced Strain Relaxation. *Phys. Rev. Lett.* **99**, 077201 (2007).
 - ¹⁹ U. Welp *et al.*, Uniaxial in-Plane Magnetic Anisotropy of $\text{Ga}_{1-x}\text{Mn}_x\text{As}$. *Appl. Phys. Lett.* **85**, 260 - 2 (2004).
 - ²⁰ Part No. PSt 150/5x5/7, from Piezomechanik, Munich, Germany.
 - ²¹ M. Shayegan *et al.*, Low-temperature, in situ tunable, uniaxial stress measurements in semiconductors using a piezoelectric actuator. *Appl. Phys. Lett.* **83**, 5235 - 7 (2003).
 - ²² D. Y. Shin *et al.*, Temperature dependence of magnetic anisotropy in ferromagnetic (Ga,Mn)As films: Investigation by the planar Hall effect. *Phys. Rev. B* **76**, 035327 (2007).

Acknowledgements The work was supported by NSF under the grants ECS-0348289 (Purdue) and DMR-0603752 (Notre Dame).